J Ginseng Res 44 (2020) 725–737

Contents lists available at ScienceDirect

Journal of Ginseng Research

journal homepage: http://www.ginsengres.org

Research Article

20(S)-Ginsenoside Rh2 displays efficacy against T-cell acute lymphoblastic leukemia through the PI3K/Akt/mTOR signal pathway

Ting Xia [1,*,☆], Jin Zhang [1,☆], Chuanxin Zhou [2], Yu Li [1], Wenhui Duan [1], Bo Zhang [1], Min Wang [1], Jianpei Fang [3,4,**]

[1] State Key Laboratory of Food Nutrition and Safety, College of Biotechnology, Tianjin University of Science & Technology, Tianjin, China
[2] Department of Pediatrics, The Fifth Hospital of Sun Yat Sen University, Sun Yat sen University, Zhuhai, Guangdong, China
[3] Department of Pediatrics, Sun Yat-sen Memorial Hospital, Sun Yat-sen University, Guangzhou, Guang Dong, China
[4] Key Laboratory of Malignant Tumor Gene Regulation and Target Therapy of Guangdong Higher Education Institutes, Sun Yat-sen University, Guangzhou, Guang Dong, China

ARTICLE INFO

Article history:
Received 26 March 2019
Received in Revised form
20 June 2019
Accepted 24 July 2019
Available online 30 July 2019

Keywords:
Apoptosis
Autophagy
Ginsenoside Rh2
PI3K/Akt/mTOR
T-cell acute lymphoblastic leukemia

ABSTRACT

Background: T-cell acute lymphoblastic leukemia (T-ALL) is a kind of aggressive hematological cancer, and the PI3K/Akt/mTOR signaling pathway is activated in most patients with T-ALL and responsible for poor prognosis. 20(S)-Ginsenoside Rh2 (20(S)-GRh2) is a major active compound extracted from ginseng, which exhibits anti-cancer effects. However, the underlying anticancer mechanisms of 20(S)-GRh2 targeting the PI3K/Akt/mTOR pathway in T-ALL have not been explored.
Methods: Cell growth and cell cycle were determined to investigate the effect of 20(S)-GRh2 on ALL cells. PI3K/Akt/mTOR pathway–related proteins were detected in 20(S)-GRh2–treated Jurkat cells by immunoblotting. Antitumor effect of 20(S)-GRh2 against T-ALL was investigated in xenograft mice. The mechanisms of 20(S)-GRh2 against T-ALL were examined by cell proliferation, apoptosis, and autophagy.
Results: In the present study, the results showed that 20(S)-GRh2 decreased cell growth and arrested cell cycle at the G1 phase in ALL cells. 20(S)-GRh2 induced apoptosis through enhancing reactive oxygen species generation and upregulating apoptosis-related proteins. 20(S)-GRh2 significantly elevated the levels of pEGFP-LC3 and autophagy-related proteins in Jurkat cells. Furthermore, the PI3K/Akt/mTOR signaling pathway was effectively blocked by 20(S)-GRh2. 20(S)-GRh2 suppressed cell proliferation and promoted apoptosis and autophagy by suppressing the PI3K/Akt/mTOR pathway in Jurkat cells. Finally, 20(S)-GRh2 alleviated symptoms of leukemia and reduced the number of white blood cells and CD3 staining in the spleen of xenograft mice, indicating antitumor effects against T-ALL *in vivo*.
Conclusion: These findings indicate that 20(S)-GRh2 exhibits beneficial effects against T-ALL through the PI3K/Akt/mTOR pathway and could be a natural product of novel target for T-ALL therapy.

1. Introduction

Acute lymphoblastic leukemia (ALL), a malignant hematologic disease, arises from proliferation of immature B or T lymphoid cells in the bone marrow. ALL is the most common malignancy in children, which occupies almost 30% of the total childhood cancers [1]. The 5-year survival for precursor B-cell ALL reaches about 80% using risk-oriented chemotherapy and supportive care, which has significant improvements in cure rates [2]. However, children with T-cell ALL (T-ALL) exhibit poor outcomes owing to chemoresistant, serious side effect and relapsed leukemia [3,4]. Therefore, it is essential to develop novel natural medicines to improve the survival rates of patients with T-ALL and minimize the side effects of conventional chemotherapy.

* Corresponding author. State Key Laboratory of Food Nutrition and Safety, Key Laboratory of Industrial Fermentation Microbiology, Ministry of Education, College of Biotechnology, Tianjin University of Science & Technology, Tianjin, 300457, PR China.
** Corresponding author. Department of Pediatrics, Sun Yat-sen Memorial Hospital, Sun Yat-sen University, Guangzhou, Guang Dong, 510120, PR China.Fax: +86 22 60602298.
E-mail addresses: xiating@tust.edu.cn (T. Xia), jpfang2005@163.com (J. Fang).
☆ These authors have contributed equally to this work.

https://doi.org/10.1016/j.jgr.2019.07.003
p1226-8453 e2093-4947/$ – see front matter

Ginseng is used as a traditional medicinal plant, which can exhibit various pharmacological effects including regulation of the central nervous system and cardiotonic, antioxidation, and antitumor effects [5–7]. Ginsenosides are derived from the roots of diverse ginseng species, which are the main bioactive components in ginseng [8]. Among the ginsenosides, ginsenoside Rh2 (GRh2) is divided into 20(S) and 20(R) according to the orientation of the hydroxyl group at the C-20 position, and 20(S)-GRh2 was found to be more effective than 20(R)-GRh2 on cancer cells [9]. Several studies have demonstrated that GRh2 exerted its antitumor activities by inhibiting cell growth and invasion and inducing apoptosis and autophagy [10,11], whereas it had no influence on normal cells [9]. However, the anticancer mechanisms of 20(S)-GRh2 against ALL cells and its underlying targeted treatment have been rarely explored.

Apoptosis is type I programmed cell death closely related to the fate of tumor [12]. Apoptosis is usually triggered by caspases and B-cell lymphoma-2 (Bcl-2) family proteins, which induces condensation and fragmentation of chromatin, formation of apoptotic bodies, and degradation of cellular constituents [13]. Autophagy is a self-balancing process by degrading damaged or superfluous organelles and macromolecules in eukaryotic cells [14]. Autophagy is essential for maintaining cellular homeostasis when cells are faced with different stresses and regulating the development of oncogenesis [15]. Autophagy and apoptosis are two crucial cellular progresses associated with complicated and interconnected protein networks, which can be regulated by some signaling pathways [16]. The PI3K/Akt/mTOR signaling pathway has been considered as a crucial regulator of autophagy and apoptosis [17,18]. It has been confirmed that activation of the PI3K/Akt/mTOR pathway was detected in 85% of patients with T-ALL, which enhanced tumorigenesis [19]. Inhibition of the PI3K/Akt/mTOR pathway has exhibited promising outcomes in different tumors, especially hematological malignancies, and might be a novel target for ALL therapy [20,21]. Whether the PI3K/Akt/mTOR pathway takes part in the anticancer effect of 20(S)-GRh2 against T-ALL is still rarely elucidated.

In the present study, we explored underlying anticancer mechanisms of 20(S)-GRh2 on T-ALL cells through determining cell cycle, apoptosis, and autophagy. Then, we investigated the therapeutic potential of 20(S)-GRh2 as a target on T-ALL cells through detecting the expression of PI3K/Akt/mTOR pathway–associated proteins. We further observed whether the PI3K/Akt/mTOR pathway was involved in 20(S)-GRh2–induced cytotoxic activity by cell proliferation, apoptosis, and autophagy. These findings would be helpful to elucidate the possible efficacy of 20(S)-GRh2 targeting the PI3K/Akt/mTOR pathway against T-ALL cells and provide a targeted agent for the precise treatment of childhood leukemia.

2. Materials and methods

2.1. Materials

20(S)-GRh2, with a purity of 99.48%, was obtained from Beijing North Carolina Chuanglian Biological Technology Research Institute (Beijing, China). Working stock solutions of 20(S)-GRh2 were prepared by dissolving compounds in dimethyl sulfoxide (DMSO; Sigma-Aldrich, Milan, Italy) before use. The final density of DMSO was $< 0.1\%$. LY294002 (PI3K inhibitor), GSK690693 (Akt inhibitor), and Rapamycin (mTOR inhibitor) were obtained from Sigma (St. Louis, MO, USA).

The primary antibodies against cytochrome *c*, cleaved caspase-3, Beclin-1, Atg5, cyclin B1, and cyclin D1 and the secondary antibodies were obtained from Cell Signaling Technology (Danvers, MA, USA). β-Actin, Bax, Bal-2, LC3, p-P70S6K, and p-4EBP1 were purchased from the Abcam company (Cambridge, MA, USA). PI3K (p85), Akt, p-Akt (Ser473), mTOR, and p-mTOR (Ser2448) were derived from Santa Cruz Biotechnology (Santa Cruz, CA, USA). The primary antibody against human CD3 was purchased from eBioscience (San Diego, CA, USA).

2.2. Cell culture

The human Reh (pre–B-cell ALL cell line) and Jurkat (T-ALL cell line) cell lines were obtained from the Cell Bank of Chinese Academy of Science (Shanghai, China) and cultured in RPMI 1640 medium (Hyclone, Logan, Utah, USA) containing 10% fetal bovine serum (Hyclone) at 37°C with 5% CO2.

2.3. Animals

Female NOD/SCID mice (3–4 weeks of age) were obtained from Beijing Vital River Laboratory Animal Technology Co., Ltd (Beijing, China). All animal protocols were performed in accordance with the guidelines of the institutional animal ethics committee and were permitted by the Institutional Animal Committee of Nankai University (SYXK 2014-0003, No. 94 Weijin Road, Nankai District, Tianjin, China). All the mice were housed in a specific pathogen-free environment under a 12-h light/12-h dark cycle. The mice were randomly divided into the control group and 20(S)-GRh2 group. All mice were treated with cyclophosphamide (100 mg/kg) for two days by intraperitoneal injection. Twenty-four hours later, Jurkat cells (5.0×10^6 cells, 200 μL volume) were administrated into the mice *via* tail vein injection. Once $\geq$1% leukemic cells were detected in the peripheral blood, 20(S)-GRh2 (40 mg/kg body weight (b.w.)) was administered once daily for three consecutive weeks by oral gavage in the 20(S)-GRh2 group. The control group received 0.1% DMSO. Body weights were measured twice a week. On Day 22, the mice were sacrificed, and the blood was collected for routine examination. The spleens were harvested for immunohistochemistry analysis.

2.4. Cell viability assays

Reh and Jurkat cells (5×10^5 in 100 μL/well) were treated without or with 35 μM 20(S)-GRh2 and PI3K/Akt/mTOR inhibitor for a required time period. DMSO groups were treated with an equal amount of DMSO (final concentration<0.1%). Then, 10 μL of Cell Counting Kit-8 solution was added to the cells at 37 °C for 4 h. Determination of absorbance was carried out using an enzyme-linked immunosorbent assay reader (Tecan, Salzburg, Austria) at 450 nm.

2.5. Cell cycle analysis

Cell cycle was measured by detecting cellular DNA content, which stained with propidium iodide (PI; BD Pharmingen, San Diego, CA, USA). 20(S)-GRh2 (0, 35 μM) was added into cells for 24 h; then, 75% cold ethanol was incubated in the culture medium at −20 °C for 1 h. Next, the samples were incubated in RNase (100 μg/ml) and irradiated at 37 °C for 30 min. At last, the cells were incubated in PI (100 μg/ml) in the dark for another 30 min. The samples were tested by flow cytometry (Becton Dickinson, CA, USA) immediately.

2.6. Analysis of nuclear morphology

20(S)-GRh2 (0, 35 μM) was added into cells for 24 h. The cells were washed with phosphate buffer solution (PBS) and incubated in 1 mg/mL Hoechst 33342 (Sigma) away from light for 3 min. Finally, the cells were measured using a fluorescence microscope (Nikon Corp., Tokyo, Japan) after washing with PBS [22].

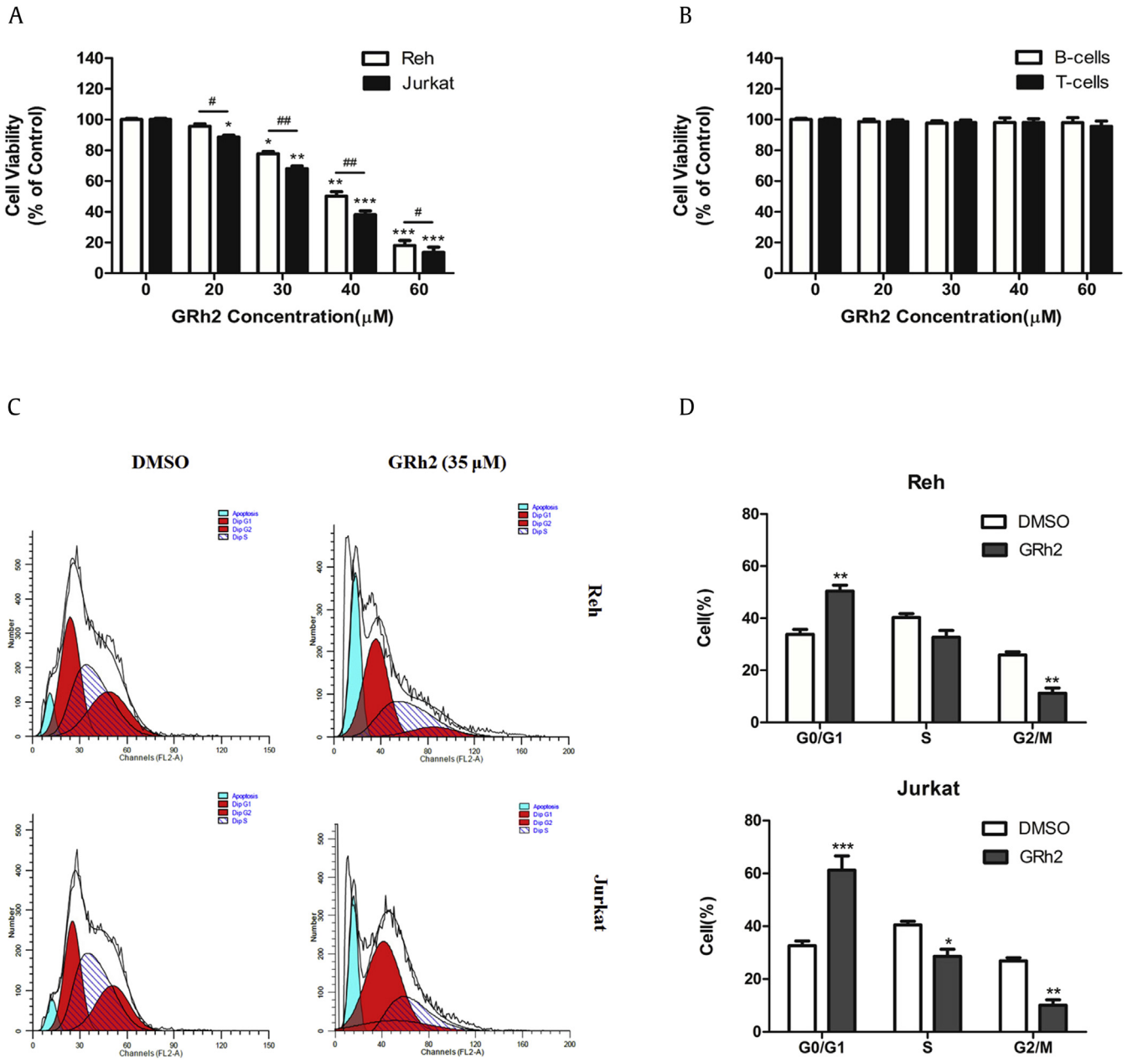

Fig. 1. 20(S)-GRh2 inhibited cell growth and arrested cell cycle in ALL cells. (A) Reh and Jurkat cells were treated with different concentrations of 20(S)-GRh2 (0, 20, 30, 40, and 60 μM) for 24 h. Cell viability was measured by Cell Counting Kit-8 assay. (B) Human normal B cells and T cells were treated with different concentrations of 20(S)-GRh2 (0, 20, 30, 40, and 60 μM) for 24 h. Cell viability was measured by CCK-8 assay. (C) Reh and Jurkat cells were treated with or without 35 μM 20(S)-GRh2 for 24 h. Cell cycle was detected by PI staining, followed by flow cytometry. (D) The percentages of ALL cells in each phase of the cell cycle (G0/G1, S, and G2/M) are shown. Data represent mean ± SD. n = 3 for each group. $^{*}p < 0.05$., $^{**}p < 0.01$, $^{***}p < 0.001$ *vs.* DMSO group. ALL, acute lymphoblastic leukemia; DMSO, dimethyl sulfoxide; GRh2, ginsenoside Rh2; PI, propidium iodide; SD, standard deviation.

2.7. Annexin V/PI flow cytometry assay

Jurkat cells were added without or with different ligands for 24 h and then incubated in 500 μL binding buffer, followed by 10 μL allophycocyanin-conjugated Annexin V and PI (BD Pharmingen) treatment away from light for 15 min. The samples were detected by flow cytometry (FACS Caliber, BD Bioscience, San Diego, CA, USA) immediately.

2.8. Detection of reactive oxygen species generation

The cells were incubated without or with 20(S)-GRh2 at different doses for 24 h. 2′,7′-Dichlorofluorescein diacetate (Sigma-Aldrich, St. Louis, MO, USA) was added into the culture medium. Next, the cells were irradiated at 37 °C away from light for 30 min. After cleaning with PBS, the fluorescence intensity of dichlorofluorescein was tested by flow cytometry immediately.

2.9. The Click-iT® 5-ethynyl-2′-deoxyuridine assay

Jurkat cells were treated with diverse ligands for 24 h. The cells were inoculated in 100 μL methanol away from light for 15 min. Click-iT® 5-ethynyl-2′-deoxyuridine was obtained from Life Technologies (Life Technologies, Grand Island, NY, USA). Five hundred microliters of the Alexa Fluor®647 fluorescence reaction mixture

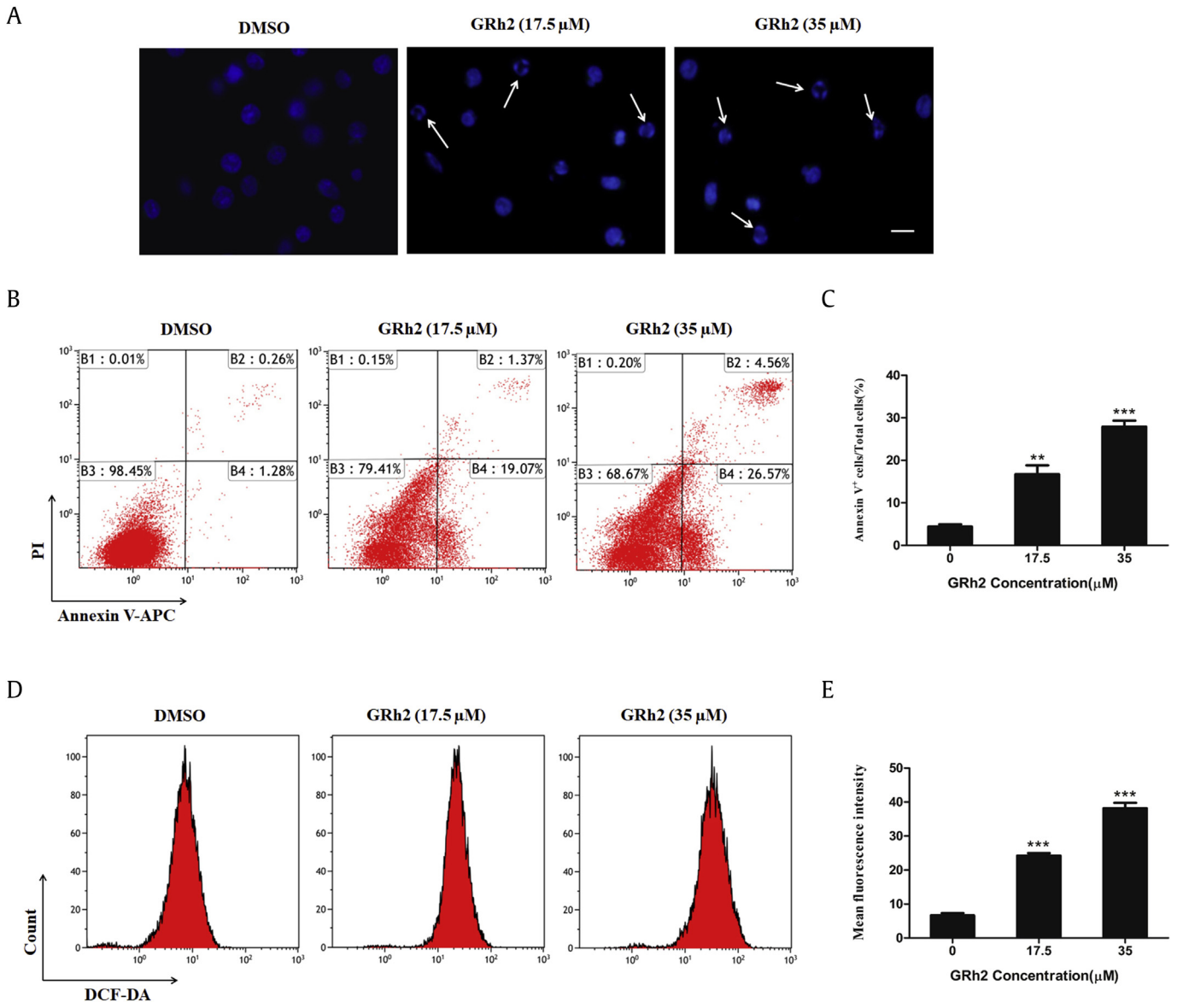

Fig. 2. 20(S)-GRh2 induced ROS-mediated apoptosis in Jurkat cells. Cells were treated with different concentrations of 20(S)-GRh2 (0, 17.5, and 35 μM) for 24 h. (A) Apoptotic cells were examined by Hoechst staining via fluorescence microscopy (Bar = 10 μM). (B) Cells were stained with Annexin V-APC and propidium iodide (PI) and detected using a flow cytometer. (C) The percentage of apoptotic cells was analyzed and quantified. (D) Cells were stained with DCFH-DA. The DFC fluorescence intensity was measured by flow cytrometry. (E) The mean fluorescence intensity was analyzed and depicted. Data represent mean ± SD. n = 3 for each group. $^{**}p < 0.01$, $^{***}p < 0.001$ *vs.* DMSO group. APC, allophycocyanin; DCFH-DA, dichlorofluorescein diacetate; DMSO, dimethyl sulfoxide; GRh2, ginsenoside Rh2; ROS, reactive oxygen species; SD, standard deviation.

was added to each sample, and the resultant was incubated for 30 min away from light. The samples were finally evaluated using flow cytometry immediately.

2.10. Detection of autophagic vacuoles by monodansylcadaverine staining

Autophagic vacuoles in Jurkat cells were detected by monodansylcadaverine (MDC) staining (Sigma). 20(S)-GRh2 (35 μM) was added to Jurkat cells (5×10^5/well) for 24 h, followed by inoculation with 50 μM MDC, an autofluorescent base capable of accumulating in autophagic vacuoles, and fixed with PBS at 37 °C for 1 h. At last, the cells were washed three times with PBS and immediately detected by flow cytometry. The autophagic index was determined as the percentage of MDC-labeled cells of 100 cells from each sample.

2.11. pEGFP-LC3 transfection

pEGFP-LC3 plasmids (Addgene plasmid 24920; Addgene, Cambridge, MA, USA) were transfected into Jurkat cells using Lipofectamine 2000 (Invitrogen, CA, USA). After transfection for 24 h, the cells were treated without or with diverse reagents for 24 h. A laser scanning confocal microscope (Zeiss, Germany) was used to observe fluorescence of GFP-LC3 in Jurkat cells. The level of autophagy was determined through counting the mean number of the punctuated pattern of green fluorescent protein (GFP) in each cell.

2.12. Transmission electron microscopy

Jurkat cells were harvested and blended with 3% glutaraldehyde solution (pH 7.4). The samples were postincubated with 1% OsO_4, followed by dehydration with ethanol (30–95%, 5 min for each

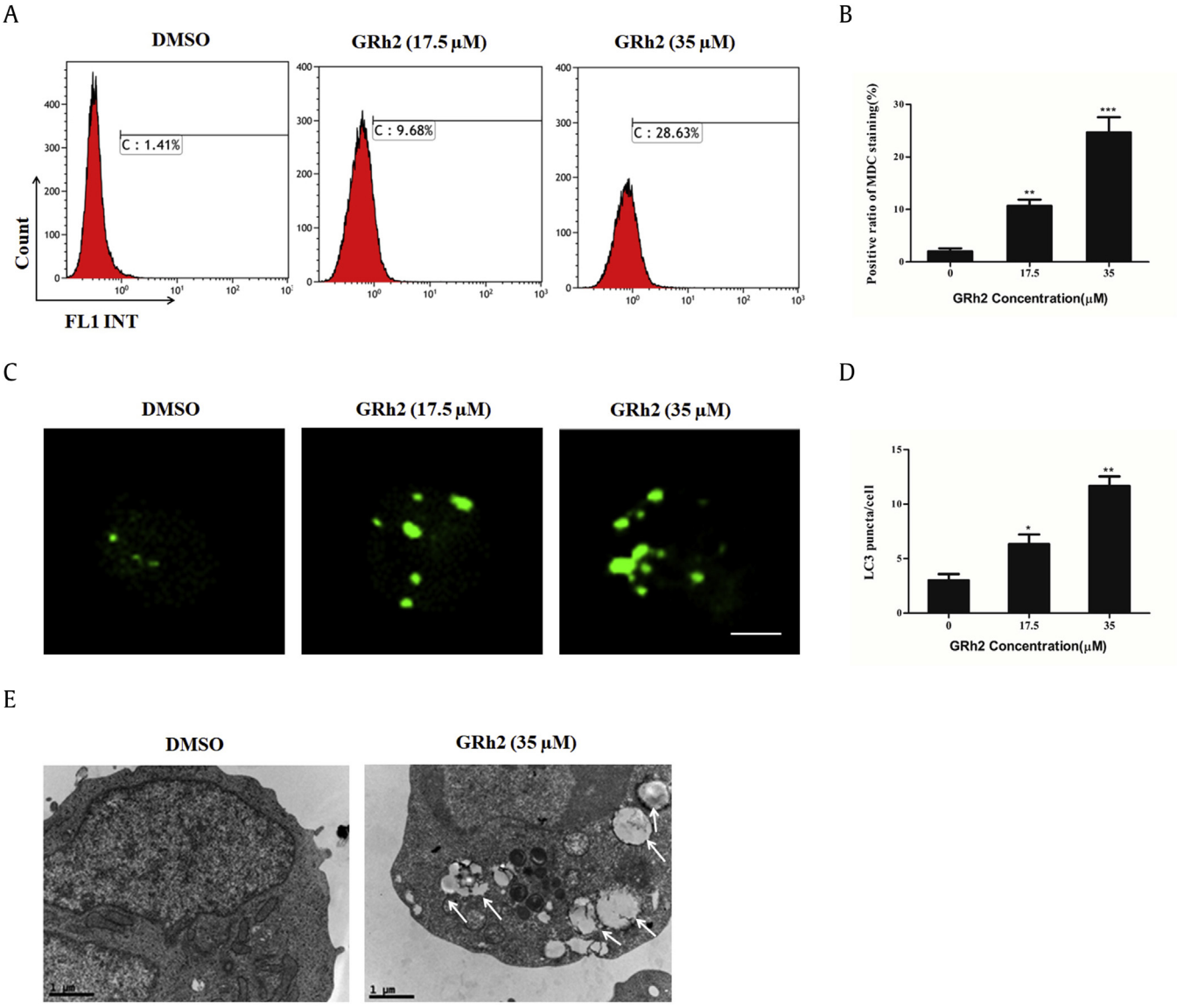

Fig. 3. 20(S)-GRh2 induced autophagy in Jurkat cells. Cells were treated with different concentrations of 20(S)-GRh2 (0, 17.5, and 35 μM) for 24 h. (A) Cells were stained with MDC, and autophagic vacuoles were detected using a flow cytometer. (B) Quantification of autophagic vacuoles in Jurkat cells. (C) The fluorescence of GFP-LC3 was observed using a laser scanning confocal microscope (bar = 5 μM). (D) The number of GFP-LC3 puncta was quantified in each cell. Quantitation represents at least 100 cells counted and scored per treatment. (E) The ultrastructure of Jurkat cells was visualized using a transmission electron microscope (bar = 5 μM). $^{*}p < 0.05$, $^{**}p < 0.01$, $^{***}p < 0.001$ *vs.* DMSO group. Autophagic vacuoles are indicated by white arrows. DMSO, dimethyl sulfoxide; GRh2, ginsenoside Rh2; MDC, monodansylcadaverine.

step). At last, the samples were incubated at 60 °C for 2 days. Finally, lead citrate and uranyl acetate were used to deal with ultrathin sections. The samples were observed by an excitation voltage of 80 kV under a Tecnai G2 Spirit Twin transmission electron microscope (FEI, Oregon, USA).

2.13. Immunoblotting analysis

The collected cells were mixed with radio immuno precipitation assay (RIPA) buffer (Sigma) for half an hour. The BCA reagent was used to examine the concentration of proteins. Proteins (20 μg) were loaded per lane and separated by 12% sodium dodecyl sulfate–polyacrylamide gel electrophoresis gel. The protein samples were transferred onto a polyvinylidene fluoride membrane (Millipore, Billerica, MA, USA) after electrophoresis. Then, the membranes were blocked with 5% milk for 1 h using TBST (20 mM Tris-HCl, 0.1% Tween 20). The membranes were irradiated at 4 °C with primary antibodies overnight. The next day, the membranes were cleaned with TBST and incubated with secondary antibodies for 1.5 h. After TBST washing, the protein membranes were washed with TBST and scanned using the Odyssey infrared imaging system (LI-COR, NE, USA) [23].

2.14. Immunohistochemistry

Immunohistochemistry was performed on the spleen of NOD/SCID mice to investigate changes in CD3 expression. The spleen tissues were incubated in 4% paraformaldehyde for 24 h. Then, the tissues were embedded into paraffin and sliced into 5-μm sections, followed by staining with CD3 antibody (1:500). The sections were placed at 4 °C overnight. The next day, the stained tissues were added with the secondary antibody (1:5000) and incubated for 2 h. After washing with PBS, the samples were scanned using a Pannoramic Scan 250 Flash (3DHISTECH Kft, Budapest, Hungary), and the images were captured using QCapture (QImaging, Burnaby, Canada) with QImaging on a Macintosh computer.

A

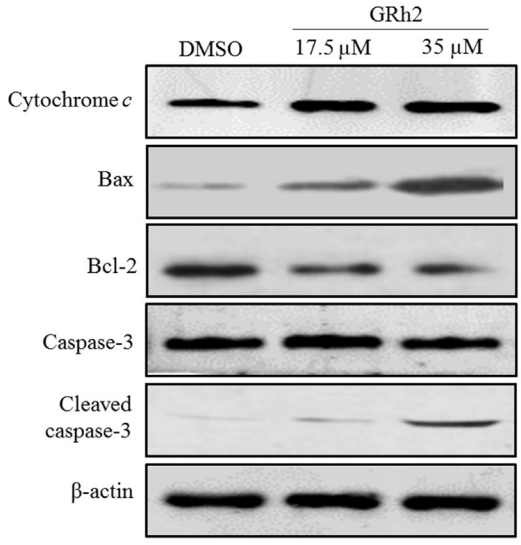
GRh2
DMSO
17.5 μM
35 μM
Cytochrome c
Bax
Bcl-2
Caspase-3
Cleaved caspase-3
β-actin

B

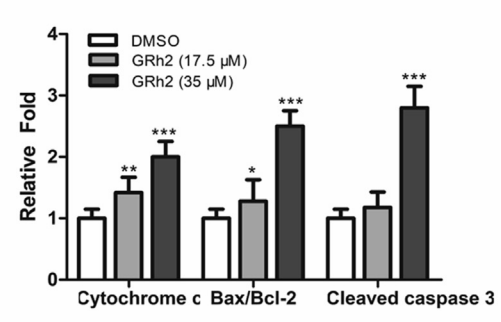
DMSO
GRh2 (17.5 μM)
GRh2 (35 μM)
Relative Fold
Cytochrome c
Bax/Bcl-2
Cleaved caspase 3

C

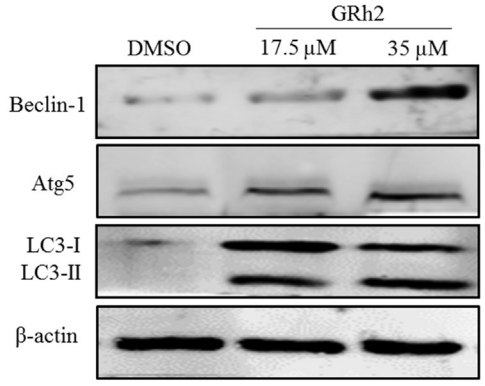
GRh2
DMSO
17.5 μM
35 μM
Beclin-1
Atg5
LC3-I
LC3-II
β-actin

D

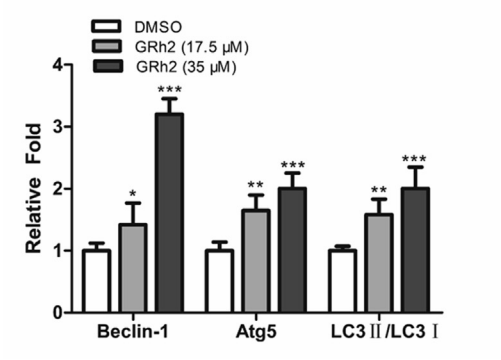
DMSO
GRh2 (17.5 μM)
GRh2 (35 μM)
Relative Fold
Beclin-1
Atg5
LC3 II /LC3 I

E

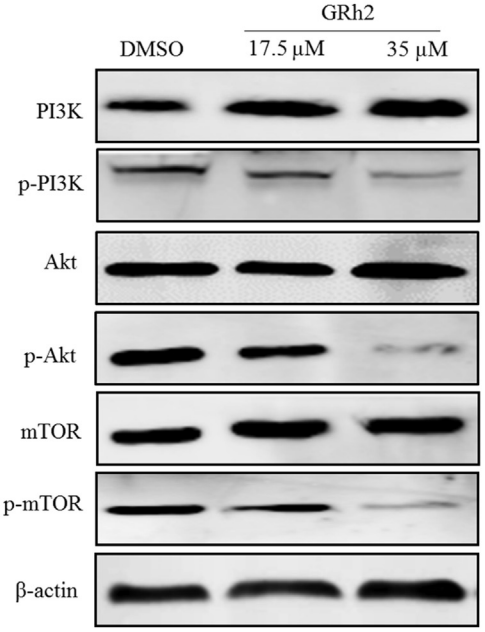
GRh2
DMSO
17.5 μM
35 μM
PI3K
p-PI3K
Akt
p-Akt
mTOR
p-mTOR
β-actin

F

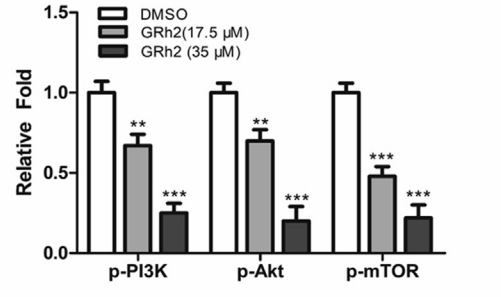
DMSO
GRh2(17.5 μM)
GRh2 (35 μM)
Relative Fold
p-PI3K
p-Akt
p-mTOR

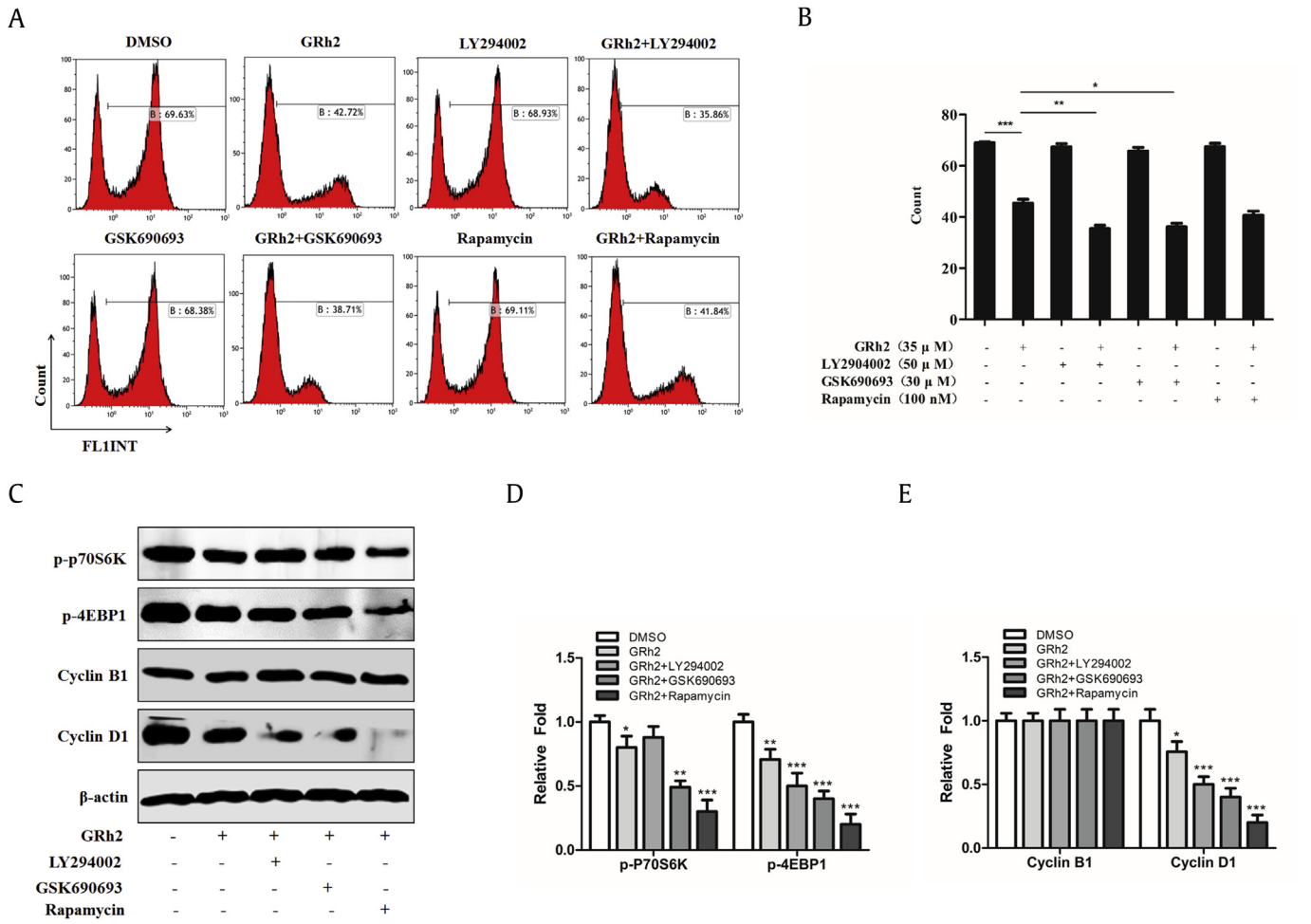

Fig. 5. 20(S)-GRh2 reduced cell proliferation via the PI3K/Akt/mTOR pathway. Jurkat cells were treated with 20(S)-GRh2 alone or combined with the PI3K/Akt/mTOR inhibitor for 24 h. (A) Cells were stained with EdU and analyzed using a flow cytometer. (B) Quantification of EdU-positive cells. (C) The expression levels of p-P70S6K, p-4EBP1, cyclin B1, and cyclin D1 were detected by Western blot analysis. (D) Quantification of p-P70S6K and p-4EBP1 expression. (E) Quantification of cyclin B1 and cyclin D1 expression. Data are expressed as mean ± SD. n = 3 for each group. $^{*}p < 0.05$, $^{**}p < 0.01$, $^{***}p < 0.001$ *vs.* DMSO group. DMSO, dimethyl sulfoxide; EdU, 5-ethynyl-2′-deoxyuridine; GRh2, ginsenoside Rh2; SD, standard deviation.

2.15. Statistical analyses

Statistical analysis was performed using Prism GraphPad 6.0 (GraphPad Software Inc., CA, USA). All of the data were expressed as the mean ± standard deviation. The one-way analysis of variance test was used to perform comparisons among all groups. Significant differences were analyzed on the basis of the Bonferroni post hoc test. A value of $p < 0.05$ was considered statistically significant.

3. Results

3.1. 20(S)-GRh2 suppressed cell growth and arrested cell cycle in ALL cells

Cell viability and cell cycle were detected to investigate the effect of 20(S)-GRh2 on ALL cells. The results showed that cell viability was significantly decreased by 30–60 μM 20(S)-GRh2 and inhibited in a concentration-dependent manner. At the same concentration, 20(S)-GRh2 inhibited cell viability more obviously in Jurkat cells than in Reh cells (Fig. 1A). However, the cell viability was not significantly decreased in normal B and T cells (Fig. 1B). In addition, the percentages of Reh and Jurkat cells in the G1 phase in 20(S)-GRh2–treated groups were 49.66 ± 6.28% and 61.22 ± 5.39%, respectively (Fig. 1C and D). 20(S)-GRh2 treatment induced a cell cycle arrest at the G1 phase compared with the DMSO treatment. Meanwhile, 20(S)-GRh2 treatment induced the increase of the cell population in the sub-G1/G1 phase, indicating the promotion of cell apoptosis. Collectively, the results indicate that 20(S)-GRh2 suppresses cell growth and arrests cell cycle at the G1 phase in ALL cells.

3.2. 20(S)-GRh2 induced reactive oxygen species–mediated apoptosis in Jurkat cells

To evaluate the effect of 20(S)-GRh2 on apoptosis, cell nuclear morphology, apoptotic cells, and reactive oxygen species (ROS)

Fig. 4. Western blot analysis of 20(S)-GRh2–treated Jurkat cells. Cells were treated with different concentrations of 20(S)-GRh2 (0, 17.5, and 35 μM) for 24 h. (A) The expression levels of Bax, Bcl-2, cytochrome *c*, and cleaved caspase-3 were detected by Western blot analysis. (B) Quantification of Bax, Bcl-2, cytochrome *c*, and cleaved caspase-3 expression. (C) The expression levels of Beclin-1, Atg5, and LC3 were analyzed by Western blot. (D) Quantification of Beclin-1, Atg5, and LC3 expression. (E) The expression levels of p-PI3K, Akt, p-Akt, mTOR, and p-mTOR were measured by Western blot analysis. (F) Quantification of p-PI3K, Akt, p-Akt, mTOR, and p-mTOR expression. Data are expressed as the mean ± SD. n = 3 for each group. $^{*}p < 0.05$, $^{**}p < 0.01$, $^{***}p < 0.001$ *vs.* DMSO group. DMSO, dimethyl sulfoxide; GRh2, ginsenoside Rh2; SD, standard deviation.

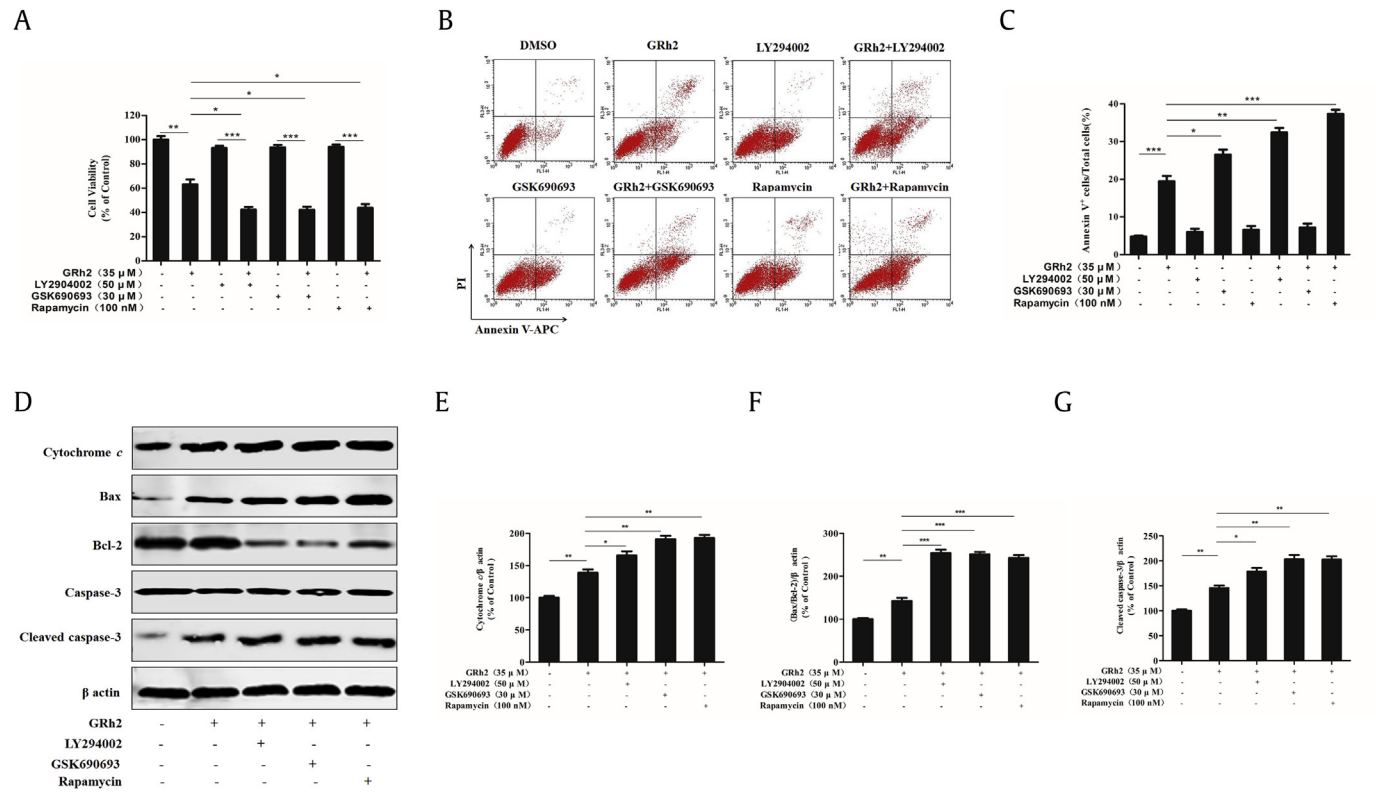

Fig. 6. 20(S)-GRh2–induced apoptosis was mediated through the PI3K/Akt/mTOR pathway. Jurkat cells were treated with 20(S)-GRh2 alone or combined with the PI3K/Akt/mTOR inhibitor for 24 h. (A) Cell viability was measured by CCK-8 assay. (B) Cells were stained with Annexin V-APC and propidium iodide (PI) and detected using a flow cytometer. (C) The percentage of apoptotic cells was analyzed and quantified. (D) The expression levels of Bax, Bcl-2, cytochrome *c*, and cleaved caspase-3 were detected by Western blot analysis. (E) Quantification of cytochrome *c* expression. (F) Quantification of Bax and Bcl-2 expression. (G) Quantification of cleaved caspase-3 expression. Data represent means of experiments ± SD. n = 3 for each group. $^{*}p < 0.05$, $^{**}p < 0.01$, $^{***}p < 0.001$ *vs.* DMSO group. APC, allophycocyanin; DMSO, dimethyl sulfoxide; GRh2, ginsenoside Rh2; SD, standard deviation.CCK-8,

levels were examined in Jurkat cells. The results showed that condensed chromatin and fragmented nucleus of Jurkat cells were clearly exhibited in the GRh2 group compared with those in the DMSO-treated group, indicating cell apoptosis. The numbers of nuclei apoptotic bodies were further increased in 35 μM 20(S)-GRh2–treated cells (Fig. 2A). The percentage of Annexin V–positive cells was 16.73 ± 3.60% in the 17.5-μM 20(S)-GRh2–treated group and further increased to 27.93 ± 2.46% in the 35-μM 20(S)-GRh2–treated group (Fig. 2B and C). Moreover, mean fluorescence intensity of dichlorofluorescein was 24.23 ± 1.31 in the 17.5-μM 20(S)-GRh2–treated group and increased to 38.16 ± 2.77 in the 35-μM 20(S)-GRh2–treated group (Fig. 2D). ROS levels in the 20(S)-GRh2 group were significantly increased in a dose-dependent manner (Fig. 2E). Taken together, the results imply that 20(S)-GRh2 promotes apoptosis through elevating ROS generation in Jurkat cells.

3.3. 20(S)-GRh2 induced autophagy in Jurkat cells

To explore the effect of 20(S)-GRh2 on autophagy in Jurkat cells, we first examined autophagic vacuoles by MDC staining. In the present study, the cells exhibited an increase in the MDC-positive ratio in the 20(S)-GRh2 group, indicating the increasing formation of the autophagic vacuoles compared with that in the DMSO-treated group (Fig. 3A and B). Accumulation of modified LC3 to the nascent autophagic vesicle is a common event in autophagosome formation [24]. We next detected the formation of the autophagosome by transmission electron microscopy. After increasing the dose of 20(S)-GRh2 treatment, GFP-LC3 punctate dots were gradually increased in Jurkat cells (Fig. 3C). In addition, 20(S)-GRh2 significantly increased the number of GFP-LC3–positive puncta per cell in a dose-dependent manner (Fig. 3D), indicating the increase of autophagosomes presented in Jurkat cells after 20(S)-GRh2 treatment.

To further confirm 20(S)-GRh2–induced autophagy, the ultrastructural alterations in Jurkat cells were analyzed. As shown in Fig. 3E, autophagic vacuoles including residual digested material or lamellar structures and empty vacuoles were observed in the 35-μM 20(S)-GRh2–treated group, indicating that 20(S)-GRh2 elevated the numbers of vacuoles and mature autophagosomes formed per cell. Collectively, the results imply that autophagy can be induced by 20(S)-GRh2 in a dose-dependent manner in Jurkat cells.

3.4. The PI3K/Akt/mTOR signaling pathway was effectively blocked by 20(S)-GRh2

Furthermore, to explore the mechanism of GRh2-induced cell death, we detected the effects of 20(S)-GRh2 on the expression of apoptosis-associated and autophagy-related proteins in Jurkat cells. The expression of cytochrome *c* and cleaved caspase-3 proteins and the ratio of Bax/Bcl-2 were increased in a dose-dependent manner after 20(S)-GRh2 treatment, implying 20(S)-GRh2 induced cell apoptosis *via* upregulation of apoptosis-associated proteins (Fig. 4A). In addition, 20(S)-GRh2 treatment obviously elevated the levels of Atg5, Beclin-1, and LC3-II (Fig. 4B), further demonstrating that 20(S)-GRh2 induced autophagy in Jurkat cells.

It is well known that the PI3K/Akt/mTOR pathway was activated in the development of the tumor, especially in patients with T-ALL [19,25]. Inhibition of this pathway is thought to be a novel target for leukemia treatment [26]. To investigate whether 20(S)-GRh2 affected this pathway, the expression of PI3K, Akt, and mTOR proteins was examined. After treatment with 20(S)-GRh2, the levels of phosphorylated PI3K, Akt, and mTOR were reduced in a dose-dependent manner (Fig. 4C). These results suggest that 20S-GRh2 can effectively inhibit the PI3K/Akt/mTOR pathway in Jurkat cells.

3.5. 20(S)-GRh2 reduced cell proliferation via inhibition of the PI3K/Akt/mTOR pathway

We used PI3K/Akt/mTOR inhibitors, LY294002, GSK690693, and rapamycin to investigate the effect of the PI3K/Akt/mTOR pathway on 20(S)-GRh2−treated Jurkat cells. As shown in Fig. 5A and B, the PI3K/Akt/mTOR inhibitor alone had no effect on cell proliferation. 20(S)-GRh2 significantly reduced the proliferation rate of Jurkat cells compared with that in the DMSO-treated group, whereas combined treatment with 20(S)-GRh2 and LY294002/GSK690693 further significantly decreased the cell proliferation rate to $35.41 \pm 2.37\%$ and $36.14 \pm 2.45\%$, respectively. The 20(S)-GRh2 and rapamycin combination had no significant decline compared with the 20(S)-GRh2 group.

We next examined the expression of proliferation-related proteins by immunoblotting. P70S6K and 4EBP1 are two key factors for cell survival and proliferation, which are the downstream targets of PI3K/Akt/mTOR [27]. As shown in Fig. 5C, 20(S)-GRh2 significantly decreased the levels of p-P70S6K and p-4EBP1 compared with the DMSO group. However, these levels were further decreased by 20(S)-GRh2 combined with the PI3K/Akt/mTOR inhibitor. Meanwhile, 20(S)-GRh2 treatment significantly decreased the level of cyclin D1, which was further reduced by combination with the PI3K/Akt/mTOR inhibitor together. However, the level of cyclin B1 was slightly affected by the combined treatment. Collectively, these findings indicate that 20(S)-GRh2 targets the PI3K/Akt/mTOR pathway, which subsequently suppresses cell proliferation and causes G1 arrest in Jurkat cells.

3.6. 20(S)-GRh2 accelerated cell apoptosis through preventing the PI3K/Akt/mTOR pathway

Then, we examined cell viability and apoptotic cells treated by 20(S)-GRh2 to investigate the effect of PI3K/Akt/mTOR pathway on apoptosis. These results showed that cell viability was significantly reduced by 20(S)-GRh2, which was further decreased after the combined treatment with 20(S)-GRh2 and PI3K/Akt/mTOR inhibitor (Fig. 6A). In addition, the percentage of apoptotic cells in the 20(S)-GRh2 group was significantly elevated compared with that in the DMSO group and was further increased in the combination group of 20(S)-GRh2 and PI3K/Akt/mTOR inhibitor (Fig. 6B and C). The PI3K/Akt/mTOR inhibitor, LY294002, GSK690693, or rapamycin alone had no obvious effect on cell viability and the apoptosis percentage of Jurkat cells.

Furthermore, we detected the expression of apoptosis-associated proteins by immunoblotting to confirm the effect of the PI3K/Akt/mTOR pathway. As shown in Fig. 6D, 20(S)-GRh2 enhanced the levels of cytochrome *c*, cleaved caspase-3, and the ratio of Bax/Bcl-2. However, these protein levels were further increased after combined treatment with 20(S)-GRh2 and PI3K/Akt/mTOR inhibitor, indicating that cell apoptosis was further aggravated. Taken together, these results imply that 20(S)-GRh2 accelerates apoptosis by preventing the PI3K/Akt/mTOR pathway in Jurkat cells.

3.7. 20(S)-GRh2 promotes autophagy by suppressing the PI3K/Akt/mTOR pathway

We also evaluated the effect of the PI3K/Akt/mTOR pathway on 20(S)-GRh2−induced autophagy in Jurkat cells. The results showed that the expression of pEGFP-LC3 in 20(S)-GRh2 and PI3K/Akt/mTOR inhibitor combination groups was further increased compared with that in the 20(S)-GRh2 group by fluorescence microscopy (Fig. 7A). Meanwhile, combination with 20(S)-GRh2 and PI3K/Akt/mTOR inhibitor further increased the number of GFP-LC3−positive puncta and autophagic grade per cell compared with 20(S)-GRh2 treatment alone (Fig. 7B and C). In addition, the levels of Beclin-1, Atg5, and LC3-I conversion to LC3-II were elevated in the 20(S)-GRh2 group compared with those in the DMSO-treated group, which were further promoted by combination with 20(S)-GRh2 and PI3K/Akt/mTOR inhibitor (Fig. 7D). The results indicate that 20(S)-GRh2 induces autophagy in Jurkat cells through blocking the PI3K/Akt/mTOR pathway.

3.8. 20(S)-GRh2 inhibits growth of Jurkat cells in xenograft mice

Antitumor effect of 20(S)-GRh2 against T-ALL was further investigated in xenograft mice. As shown in Fig. 8A, listless inactivity, dull hair, and weight loss were observed in SCID/NOD mice after inoculation with Jurkat cells. However, these symptoms were relieved by 20(S)-GRh2 treatment. In addition, body weight of xenograft mice was gradually decreased in a time-dependent manner, whereas that was reversed by 20(S)-GRh2 treatment (Fig. 8B). Furthermore, the blood routine test results showed that the number of white blood cells in the 20(S)-GRh2−treated group was significantly decreased compared with that in xenograft mice (Fig. 8C). Finally, we investigated the antitumor effect of 20(S)-GRh2 by immunohistochemical analysis. As shown in Fig. 8D, large amount of CD3 (yellow staining) was observed in xenograft mice, indicating massive accumulation of Jurkat cells in spleen tissues. However, those were markedly reduced by 20(S)-GRh2 treatment. Taken together, our results imply that 20(S)-GRh2 exhibits antitumor effects against T-ALL *in vivo*.

4. Discussion

ALL is the most common type of cancers in children, which remains the leading cause of childhood cancer death [28]. T-ALL is an aggressive hematological cancer, and the outcome of patients with T-ALL still remains a major clinical challenge [21]. Therefore, innovative strategies should be developed to further improve survival rates and reduce adverse effects of chemotherapy. Several studies reported that the PI3K/Akt/mTOR pathway plays a crucial role in T-ALL pathogenesis because the most common mutations in patients with T-ALL often lead to constitutive activation of this pathway [21,29]. GRh2 is a major active compound extracted from ginseng, which displays efficient bioactivities against several human tumors [30−32]. In this study, we explored the antileukemia effect of 20(S)-GRh2 *in vitro* and *in vivo*. Furthermore, the underlying molecular mechanisms of 20(S)-GRh2 against T-ALL were investigated. The results showed that the PI3K/Akt/mTOR signaling pathway could be effectively blocked by 20(S)-GRh2 in Jurkat cells. Our results suggest that the therapeutic potential of 20(S)-GRh2 act as a targeted drug against T-ALL.

Previous studies have found that GRh2 displayed an evident anticancer activity through suppressing cell proliferation and inducing apoptosis in tumor cells [23,33,34]. In the present study, the results showed that 20(S)-GRh2 decreased cell viability in a concentration-dependent manner in ALL cell lines and inhibited proliferation of Jurkat cells more potently than that of Reh cells.

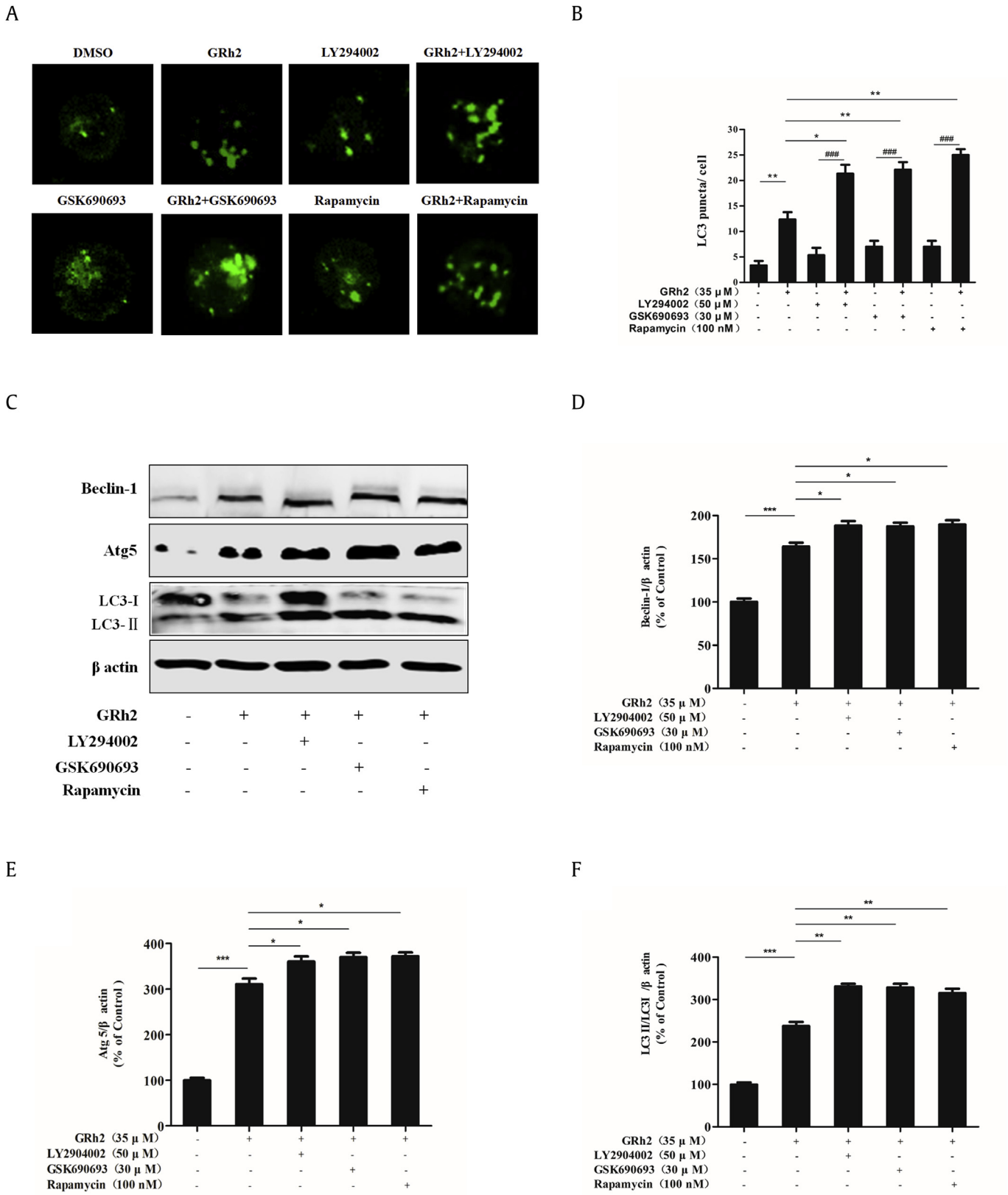

Fig. 7. 20(S)-GRh2 promoted autophagy by the PI3K/Akt/mTOR pathway. Jurkat cells were treated with 20(S)-GRh2 alone or combined with the PI3K/Akt/mTOR inhibitor for 24 h. (A) Detection of pEGFP-LC3 using a laser scanning confocal microscope (bar = 5 μM). (B) Quantification of GFP-LC3 puncta per cell. Quantitation represents at least 100 cells counted and scored per treatment. (C) The expression levels of Beclin-1, Atg5, and LC3 were analyzed by Western blot. (D) Quantification of Beclin-1 expression. (E) Quantification of Atg5 expression. (F) Quantification of LC3 expression. Data are expressed as mean ± SD. n = 3 for each group. $^{*}p < 0.05$, $^{**}p < 0.01$, $^{***}p < 0.001$ *vs.* DMSO group. $^{\#\#\#}p < 0.001$ *vs.* 20(S)-GRh2 and PI3K/Akt/mTOR inhibitor combination group. DMSO, dimethyl sulfoxide; GRh2, ginsenoside Rh2; SD, standard deviation.

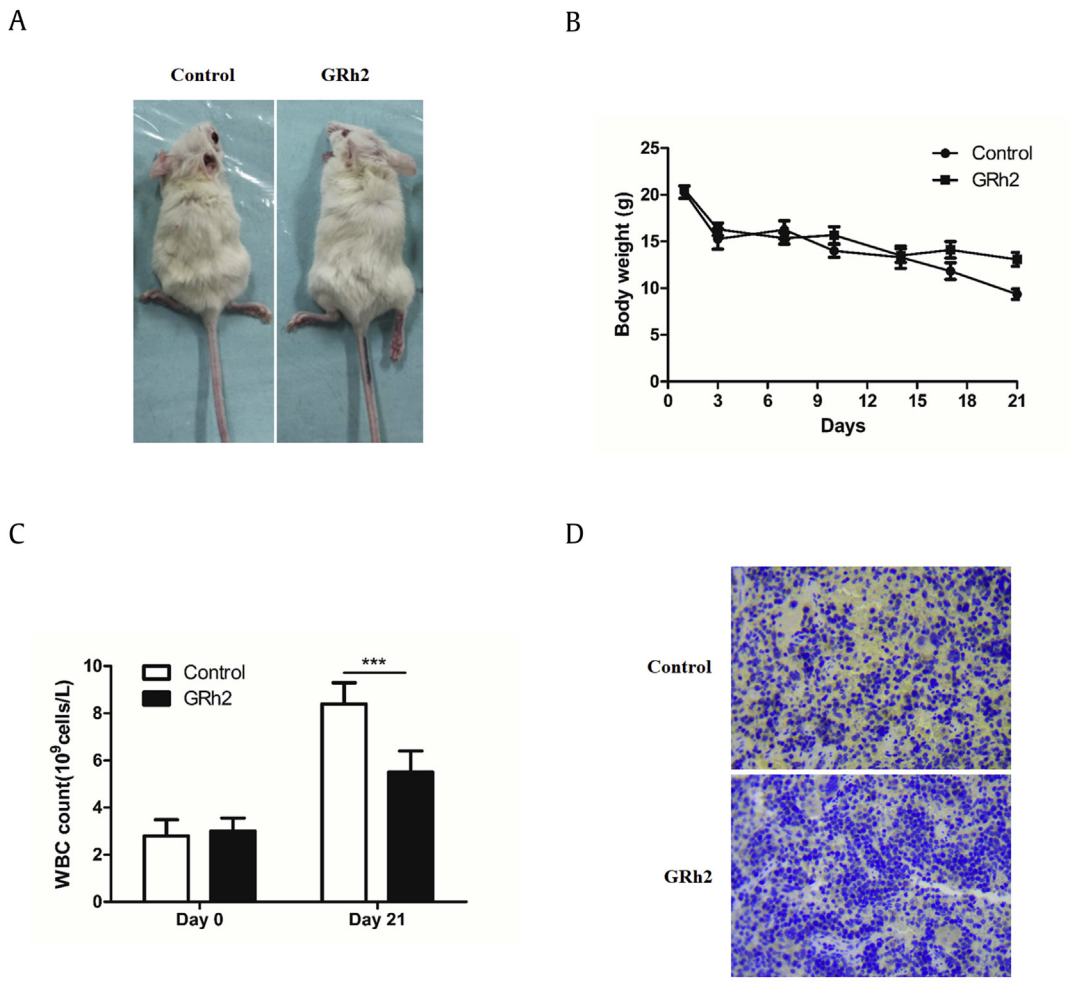

Fig. 8. The antitumor effect of 20(S)-GRh2 in xenograft mice. NOD/SCID mice were inoculated with Jurkat cells and were treated with or without 20(S)-GRh2 for 21 days. (A) Photographs of xenograft mice in the control group and 20(S)-GRh2–treated group. (B) Body weight changes in the control group and 20(S)-GRh2-treated group. (C) White blood cell count of peripheral blood in xenograft mice. (D) Immunohistochemistry analysis of the spleen for human CD3 antibody; samples were photographed at 200 × magnification. GRh2, ginsenoside Rh2; WBC, white blood cell.

Meanwhile, 20(S)-GRh2 arrested cell cycle at the G1 phase in ALL cells. Furthermore, 20(S)-GRh2 inhibited growth of Jurkat cells and CD3 infiltration in xenograft mice, indicating its antitumor effect against T-ALL *in vivo*.

It is well known that excess ROS generation in mitochondria leads to mitochondrial damage, which subsequently causes the release of proapoptotic substances from mitochondria, ultimately inducing cell apoptosis [35]. Our results found that 20(S)-GRh2 induced ROS generation, increased the numbers of nuclei apoptotic bodies and the percentage of apoptotic cells. Meanwhile, Western blot analysis showed that 20(S)-GRh2 increased the expression of cytochrome *c* and cleaved caspase-3 and the Bax/Bcl-2 ratio, which caused apoptosis in T-ALL cells. Taken together, our findings suggest that 20(S)-GRh2 can induce ROS-mediated apoptosis in Jurkat cells.

Autophagy is a process of physiological cell death that is characterized by the accumulation of autophagic vacuoles [36]. Autophagy also plays an essential role in tumor development and advancement including both tumor cell survival and death [37]. In the present study, we found that 20(S)-GRh2 significantly increased the number of autophagic vacuoles and autophagosome formation in T-ALL cells. The increased levels of autophagy-related proteins including Beclin-1, Atg5, and LC3-II are commonly used as markers for evaluating autophagy [38]. In the present study, the results showed that the levels of Beclin-1, Atg5, and LC3-II were upregulated after 20(S)-GRh2 treatment, further demonstrating that autophagic flux was enhanced in the 20(S)-GRh2–treated group.

The PI3K/Akt/mTOR signaling pathway plays an essential role in regulating cell survival and death, especially in the progression of cancer [39]. Much evidence has demonstrated that the PI3K/Akt/mTOR pathway is constitutively activated in diverse types of cancer, targeting the effectors of this pathway is a potential therapeutic approach [40,41]. Lonetti et al. [42] reported that the PI3K/Akt/mTOR pathway was activated in patients with T-ALL, and inhibitors targeting this pathway can improve efficacy of chemotherapy in T-ALL. In the present study, the levels of phosphorylated PI3K, Akt, and mTOR were downregulated by 20(S)-GRh2 in dose-dependent manners. The results first demonstrate that the PI3K/Akt/mTOR signaling pathway takes part in the anticancer effect of 20(S)-GRh2 against T-ALL cells.

The PI3K/Akt/mTOR signaling pathway is essential in regulating cell growth and survival of physiological and pathological conditions [43]. This pathway plays a key role in cell proliferation through affecting the activity of downstream effector molecules and is closely related to the development and progression of cancer [44]. However, the roles of the PI3K/Akt/mTOR pathway and its downstream components have not been explored in the 20(S)-GRh2 group. In the present study, 20(S)-GRh2

significantly decreased the proliferation rate of Jurkat cells, and combined treatment with 20(S)-GRh2 and PI3K/Akt/mTOR inhibitor further decreased cell proliferation. 4EBP1 and p70S6K, as PI3K/Akt/mTOR downstream targets, are crucial factors for proliferation in cancer cells [45]. We found that 20(S)-GRh2 combined with the PI3K/Akt/mTOR inhibitor further downregulated the levels of p-4EBP1 and p-p70S6K compared with 20(S)-GRh2 alone, which subsequently inhibited cell proliferation. The previous study has demonstrated that the PI3K/Akt/mTOR signaling pathway displayed a crucial effect in the progression of cell cycle in human prostate cancer cells [46]. G1 phase arrest resulted from the inhibition of cyclin D1 function, while G2/M phase regulation principally relied on cyclin B protein [47]. The results displayed that 20(S)-GRh2 significantly downregulated the expression of cyclin D1 protein, and the combination with the PI3K/Akt/mTOR inhibitor further reduced this level, indicating 20(S)-GRh2 arrested cell cycle at the G1 phase *via* the PI3K/Akt/mTOR pathway. Taken together, the results indicate that 20(S)-GRh2 suppresses cell cycle and proliferation by blocking the PI3K/Akt/mTOR pathway in Jurkat cells.

Apoptosis and autophagy, as catabolic pathways in various physiopathological processes, decide the fate of cancer cells [48]. mTOR is a key kinase downstream of PI3K/Akt, which regulates apoptosis and autophagy of tumor cells [49]. The PI3K/Akt/mTOR signaling pathway plays a vital role in the development of T-ALL, and inhibition of this pathway can promote cell apoptosis and autophagy [50]. It was reported that suppression of PI3K/Akt/mTOR signaling involved in releasing cytochrome *c* and activating caspase-dependent apoptosis [51]. In the present study, we found that 20(S)-GRh2 combined with the PI3K/Akt/mTOR inhibitor further decreased cell viability and elevated the number of apoptotic cells and the levels of apoptosis-associated proteins. In addition, inhibition of mTOR was also induced the elevation of the Beclin-1 level and LC3-II/LC3-I ratio in cancer cells [52]. The results displayed that the expression of pEGFP-LC3 and autophagy-related proteins were activated by 20(S)-GRh2, and those were further enhanced by the combination of 20(S)-GRh2 and PI3K/Akt/mTOR inhibitor. The results demonstrate that 20(S)-GRh2 induces apoptosis and autophagy through blocking the PI3K/Akt/mTOR pathway in Jurkat cells.

In conclusion, this study revealed that 20(S)-GRh2 displayed conspicuous anticancer effect against T-ALL cells by arresting cell cycle, inhibiting cell growth, and enhancing apoptosis and autophagy. In addition, 20(S)-GRh2 exhibited antitumor effect against T-ALL in xenograft mice. Furthermore, the anticancer mechanism of 20(S)-GRh2 was associated with targeting the PI3K/Akt/mTOR pathway to inhibit proliferation and promote apoptosis and autophagy in human T-ALL cells. These findings suggest that 20(S)-GRh2 is a natural resource of anticancer drug targeting the PI3K/Akt/mTOR pathway, and this should be evaluated in clinical trials in future.

Conflicts of interest

All authors declare no conflict of interest.

Acknowledgments

This work was supported by the National Natural Science Foundation of China (81600126, 81570140), the National Key R&D Program of China (2016YFD0400505) and Tianjin Municipal Science and Technology Commission (18PTSYJC00140).

Appendix A. Supplementary data

Supplementary data to this article can be found online at https://doi.org/10.1016/j.jgr.2019.07.003.

References

[1] Hunger SP, Mullighan CG. Redefining ALL classification: toward detecting high-risk ALL and implementing precision medicine. Blood 2015;125:3977–87.
[2] Winter SS, Sweatman J, Shuster JJ, Link MP, Amylon MD, Pullen J, Camitta BM, Larson RS. Bone marrow stroma-supported culture of T-lineage acute lymphoblastic leukemic cells predicts treatment outcome in children: a pediatric oncology group study. Leukemia 2002;16:1121–6.
[3] Matloub Y, Stork L, Asselin B, Matloub Y, Stork L, Asselin B, Hunger SP, Borowitz M, Jones T, Bostrom B, et al. Outcome of children with standard-risk T-lineage acute lymphoblastic leukemia-comparison among different treatment strategies. Pediatr Blood Cancer 2015;63:255–61.
[4] Preijers FW, De WT, Wessels JM, De Gast GC, Van Leeuwen E, Capel PJ, Haanen C. Autologous transplantation of bone marrow purged in vitro with anti-CD7-(WT1-) ricin A immunotoxin in T-cell lymphoblastic leukemia and lymphoma. Blood 1989;74:1152–8.
[5] Jin KH, Pitna K, Young SC. A comprehensive review of the therapeutic and pharmacological effects of ginseng and ginsenosides in central nervous system. J Ginseng Res 2013;37:8–29.
[6] Poindexter BJ, Allison AW, Bick RJ, Dasqupta A. Ginseng: cardiotonic in adult rat cardiomyocytes, cardiotoxic in neonatal rat cardiomyocytes. Life Sci 2006;79:2337–44.
[7] Keum YS, Park KK, Lee JM, Chun KS, Park JH, Seung KL, Kwon H, Surh YJ. Antioxidant and anti-tumor promoting activities of the methanol extract of heat-processed ginseng. Cancer Lett 2000;150:41–8.
[8] Liang Y, Zhao S. Progress in understanding of ginsenoside biosynthesis. Plant Biol 2008;10:415–21.
[9] Han S, Jeong AJ, Yang H, Kang KB, Lee H, Yi EH, Kim BH, Cho CH, Chung JW, Sung SH, et al. Ginsenoside 20(S)-Rh2 exerts anti-cancer activity through targeting IL-6-induced JAK2/STAT3 pathway in human colorectal cancer cells. J Ethnopharmacol 2016;194:83–90.
[10] Tang XP, Tang GD, Fang CY, Liang ZH, Zhang LY. Effects of ginsenoside Rh2 on growth and migration of pancreatic cancer cells. World J Gastroenterol 2013;19:1582–92.
[11] Zhuang J, Yin J, Xu C, Mu Y, Lv S. 20(S)-Ginsenoside Rh2 induce the apoptosis and autophagy in U937 and K562 cells. Nutrients 2018;10:328.
[12] Ouyang L, Shi Z, Zhao S, Wang FT, Zhou TT, Liu B, Bao JK. Programmed cell death pathways in cancer: a review of apoptosis, autophagy and programmed necrosis. Cell Prolif 2012;45:487–98.
[13] Hengartner MO. The biochemistry of apoptosis. Nature 2000;407:770–6.
[14] Klionsky DJ. Autophagy: from phenomenology to molecular understanding in less than a decade. Nat Rev Mol Cell Biol 2007;8:931–7.
[15] Gurusamy N, Lekli I, Gherghiceanu M, Popescu LM, Das DK. BAG-1 induces autophagy for cardiac cell survival. Autophagy 2009;5:120–1.
[16] Mukhopadhyay S, Panda PK, Sinha N, Das DN, Bhutia SK. Autophagy and apoptosis: where do they meet? Apoptosis 2014;19:555–66.
[17] Saiki S, Sasazawa Y, Imamichi Y, Kawajiri S, Fujimaki T, Tanida I, Kobayashi H, Sato F, Sato S, Ishikawa K, et al. Caffeine induces apoptosis by enhancement of autophagy via PI3K/Akt/mTOR/p70S6K inhibition. Autophagy 2011;7:176–87.
[18] Zhao ZQ, Zhong-Yang YU, Jie LI, Ouyang XN. Gefitinib induces lung cancer cell autophagy and apoptosis via blockade of the PI3K/AKT/mTOR pathway. Oncol Lett 2016;12:63–8.
[19] Silva A, Yunes JY, Cardoso BA, Martins LR, Jotta PY, Abecasis M, Nowill NE, Leslie NR, Cardoso AA, Barata JT. PTEN posttranslational inactivation and hyperactivation of the PI3K/Akt pathway sustain primary T cell leukemia viability. J Clin Invest 2008;118:3762–74.
[20] Neri LM, Cani A, Martelli AM, Simioni C, Junghanss C, Tabellini G, Ricci F, Tazzari PL, Pagliaro P, McCubrey JA, et al. Targeting the PI3K/Akt/mTOR signaling pathway in B-precursor acute lymphoblastic leukemia and its therapeutic potential. Leukemia 2014;28:739–48.
[21] Gazi M, Moharram SA, Marhäll A, JU Kazi. The dual specificity PI3K/mTOR inhibitor PKI-587 displays efficacy against T-cell acute lymphoblastic leukemia (T-ALL). Cancer Lett 2017;392:9–16.
[22] Xia T, Wang JC, Xu W, Xu LH, Lao CH, Ye QX, Fang JP. 20S-Ginsenoside Rh2 induces apoptosis in human Leukaemia Reh cells through mitochondrial signaling pathways. Biol Pharm Bull 2014;37:248–54.
[23] Xia T, Wang YN, Zhou CX, Wu LM, Liu Y, Zeng QH, Zhang XL, Yao JH, Wang M, Fang JP. Ginsenoside Rh2 and Rg3 inhibit cell proliferation and induce apoptosis by increasing mitochondrial reactive oxygen species in human leukemia Jurkat cells. Mol Med Rep 2017;15:3591–8.
[24] Kabeya Y, Mizushima N, Ueno T, Yamamoto A, Kirisako T, Noda T, Kominami E, Ohsumi T, Yoshimori Y. LC3/a mammalian homolog of yeast Apg8p, is localized in autophagosome membranes after processing. Embo J 2000;19:15720–8.
[25] Kim EH, Sohn S, Kwon HJ, Kim SU, Kim MJ, Lee SJ, Choi KS. Sodium selenite induces superoxide-mediated mitochondrial damage and subsequent autophagic cell death in malignant glioma cells. Cancer Res 2007;67:6314–24.

[26] Bertacchini J, Heidari N, Mediani L, Capitani S, Shahjahani M, Ahmadzadeh A, Saki N. Targeting PI3K/AKT/mTOR network for treatment of leukemia. Cell Mol Life Sci 2015;72:2337–47.
[27] Fingar DC, Salama S, Tsou C, Harlow E, Blenis J. Mammalian cell size is controlled by mTOR and its downstream targets S6K1 and 4EBP1/eIF4E. Genes Dev 2002;16:1472–87.
[28] Parker C, Waters R, Leighton C, Hancock J, Sutton R, Moorman AV, Ancliff P, Morgan M, Masurekar A, Goulden N, et al. Effect of mitoxantrone on outcome of children with first relapse of acute lymphoblastic leukaemia (ALL R3): an open-label randomised trial. Lancet 2010;376:2009–17.
[29] Silva A, Gírio A, Cebola I, Santos CI, Antunes F, Barata GT. Intracellular reactive oxygen species are essential for PI3K/Akt/mTOR-dependent IL-7-mediated viability of T-cell acute lymphoblastic leukemia cells. Leukemia 2011;39:960–7.
[30] Choi S, Kim TW, Singh SV. Ginsenoside Rh2-mediated G1 phase cell cycle arrest in human breast cancer cells is caused by p15 Ink4B and p27 Kip1-dependent inhibition of cyclin-dependent kinases. Pharm Res 2009;26:2280–8.
[31] An IS, An S, Kwon KJ, Kim YJ, Bae S. Ginsenoside Rh2 mediates changes in the microRNA expression profile of human non-small cell lung cancer A549 cells. Oncol Rep 2013;29:523–8.
[32] Li B, Zhao J, Wang CZ, Searle J, He TC, Yuan CS, Du W. Ginsenoside Rh2 induces apoptosis and paraptosis-like cell death in colorectal cancer cells through activation of p53. Cancer Lett 2011;301:185–92.
[33] Cheng CC, Yang SM, Huang CY, Chen JC, Chang WM, Hsu SL. Molecular mechanisms of ginsenoside Rh2-mediated G1 growth arrest and apoptosis in human lung adenocarcinoma A549 cells. Cancer Chemoth Pharm 2005;55:531–40.
[34] Yang J, Yuan D, Xing T, Su H, Zhang S, Wen J, Bai Q, Dang D. Ginsenoside Rh2 inhibiting HCT116 colon cancer cell proliferation through blocking PDZ-binding kinase/T-LAK cell-originated protein kinase. J Ginseng Res 2016;40:400–8.
[35] Bayir H, Kagan VE. Bench-to-bedside review: mitochondrial injury, oxidative stress and apoptosis - there is nothing more practical than a good theory. Crit Care 2008;12:206.
[36] Mizushima N, Levine B, Cuervo AM, Klionsky DJ. Autophagy fights disease through cellular self-digestion. Nature 2011;451:1069–75.
[37] Degenhardt K, Mathew R, Beaudoin B, Bray K, Anderson D, Chen G, Mukherjee C, Shi Y, Gélinas C, Fan Y, et al. Autophagy promotes tumor cell survival and restricts necrosis, inflammation, and tumorigenesis. Cancer Cell 2006;10:51–64.
[38] Aparicio IM, Espino J, Bejarano I, Gallardo-Soler A, Campo ML, Salido GM, Pariente JA, Peña FJ, Tapia JA. Autophagy-related proteins are functionally active in human spermatozoa and may be involved in the regulation of cell survival and motility. Sci Rep 2016;6:33647.
[39] Lien EC, Lyssiotis CA, Cantley LC. Metabolic reprogramming by the PI3K-Akt-mTOR pathway in cancer. Recent Results Cancer Res 2016;207:39–72.
[40] Jr PJ, Janku F. Molecular targets for cancer therapy in the PI3K/AKT/mTOR pathway. Pharmacol Ther 2014;142:164–75.
[41] Morgensztern D, Mcleod HL. PI3K/Akt/mTOR pathway as a target for cancer therapy. Anti-cancer Drug 2005;16:797–803.
[42] Lonetti A, Cappellini A, Bertaina A, Locatelli F, Pession A, Buontempo F, Evangelisti C, Evangelisti C, Orsini E, Zambonin L, et al. Improving nelarabine efficacy in T cell acute lymphoblastic leukemia by targeting aberrant PI3K/AKT/mTOR signaling pathway. J Hematol Oncol 2016;9:114.
[43] Keppler-Noreuil KM, Parker VE, Darling TN, Martinez-Agosto JA. Somatic overgrowth disorders of the PI3K/AKT/mTOR pathway & therapeutic strategies. Am J of Med Genet C Semin Med Genet 2016;172:402–21.
[44] Yu JS, Cui W. Proliferation, survival and metabolism: the role of PI3K/AKT/mTOR signalling in pluripotency and cell fate determination. Development 1991;143:3050–60.
[45] Heinonen H, Nieminen A, Saarela M, Kallioniemi A, Klefström J, Hautaniemi S, Monni O. Deciphering downstream gene targets of PI3K/mTOR/p70S6K pathway in breast cancer. BMC Genomics 2008;9:348.
[46] Gao N, Zhang Z, Jiang BH, Shi X. Role of PI3K/AKT/mTOR signaling in the cell cycle progression of human prostate cancer. Biochem Biophys Res Commun 2003;310:1124–32.
[47] Sui T, Li MA, Bai X, Li Q, Xu X. Resveratrol inhibits the phosphatidylinositide 3-kinase/protein kinase B/mammalian target of rapamycin signaling pathway in the human chronic myeloid leukemia K562 cell line. Oncol Lett 2014;7:2093–8.
[48] Hsieh YC, Athar M, Chaudry IH. When apoptosis meets autophagy: deciding cell fate after trauma and sepsis. Trends Mol Med 2009;15:129–38.
[49] Zhang L, Wang H, Zhu J, Ding K. Mollugin induces tumor cell apoptosis and autophagy via the PI3K/AKT/mTOR/p70S6K and ERK signaling pathways. Biochem Bioph Res Co 2014;450:247–54.
[50] Sanda T, Li X, Gutierrez A, Ahn Y, Neuberg DS, O'Neil J, Strack PR, Winter SS, Winter CG, Larson RS, et al. Interconnecting molecular pathways in the pathogenesis and drug sensitivity of T-cell acute lymphoblastic leukemia. Blood 2010;115:1735–45.
[51] Shrivastava S, Kulkarni P, Thummuri D, Jeengar MK, Naidu VG, Alvala M, Redddy GB, Ramakrishna S. Piperlongumine, an alkaloid causes inhibition of PI3 K/Akt/mTOR signaling axis to induce caspase-dependent apoptosis in human triple-negative breast cancer cells. Apoptosis 2014;19:1148–64.
[52] Chagin AS. Effectors of mTOR-autophagy pathway: targeting cancer, affecting the skeleton. Curr Opin Pharmacol 2016;28:1–7.